Published in final edited form as:
Magn Reson Med. 2013 September ; 70(3): 851–858. doi:10.1002/mrm.24514.

Accelerated Aortic Flow Assessment with Compressed Sensing With and Without Use of the Sparsity of the Complex Difference Image

Yongjun Kwak[1,3], **Seunghoon Nam**[1,3], **Mehmet Akçakaya**[1], **Tamer A. Basha**[1], **Beth Goddu**[1], **Warren J. Manning**[1,2], **Vahid Tarokh**[3], and **Reza Nezafat**[1]

[1]Department of Medicine (Cardiovascular Division), Harvard Medical School and Beth Israel Deaconess Medical Center, Boston, MA

[2]Department of Radiology, Harvard Medical School and Beth Israel Deaconess Medical Center, Boston, MA

[3]School of Engineering and Applied Sciences, Harvard University, Cambridge, MA

Abstract

Phase contrast (PC) cardiac MR (CMR) is widely used for the clinical assessment of blood flow in cardiovascular disease. One of the challenges of PC CMR is the long scan time which limits both spatial and temporal resolution. Compressed sensing (CS) reconstruction with accelerated PC acquisitions is a promising technique to increase the scan efficiency. In this study, we sought to utilize the sparsity of the complex difference (CD) of the two flow-encoded images as an additional constraint term to improve the CS reconstruction of the corresponding accelerated PC data acquisition. Using retrospectively under-sampled data, the proposed reconstruction technique was optimized and validated *in-vivo* on 15 healthy subjects. Then, prospectively under-sampled data was acquired on 11 healthy subjects and reconstructed with the proposed technique. The results show that there is good agreement between the cardiac output measurements from the fully-sampled data and the proposed CS reconstruction method using CD sparsity up to acceleration rate 5. In conclusion, we have developed and evaluated an improved reconstruction technique for accelerated PC CMR that utilizes the sparsity of the CD of the two flow-encoded images.

Keywords

phase contrast MR; blood flow assessment; compressed sensing; accelerated imaging; cardiac MR

INTRODUCTION

Phase contrast (PC) cardiac MR (CMR) is commonly used clinically for the *in-vivo* assessment of blood flow in cardiovascular disease (1-3). Through-plane aortic and pulmonic blood flow are measured and used for the evaluation of cardiac function and

Correspondence to: Reza Nezafat, Ph.D., Beth Israel Deaconess Medical Center, 330 Brookline Ave, Boston, MA, 02215, Phone: 617-667-1747; Fax: 617-975-5480, rnezafat@bidmc.harvard.edu.

output, mitral regurgitation, and shunts. Clinically, a through-plane 2D acquisition is performed for the evaluation of blood flow. Recent advances have also enabled 3D time-resolved PC CMR that allows quantification and visualization of the blood flow in all three directions (4). For quantitative cardiac indices such as cardiac output or mitral regurgitation, flow measurements should be accurate and reproducible. However, despite the potential of PC CMR as an alternative to Doppler ultrasound for evaluation of these indices, its accuracy is impacted by several limitations including background offset, Eddy currents, and a long scan time.

Several acquisition methods have been used to improve the data acquisition efficiency and reduce the total scan time in PC CMR. Echo planar imaging has been used to improve the temporal resolution of flow imaging (5). Non-Cartesian k-space trajectories including spiral and radial sequences have also been used to reduce scan time (6-8). Parallel imaging (9,10), which has been widely used clinically for accelerated imaging, was shown to provide accurate flow measurements with reduced scan times (11). The study by Baltes et al. (12) showed k-t BLAST and k-t SENSE are promising approaches for high-resolution breath-hold flow quantification through the ascending aorta with up to 5-fold acceleration. To overcome the limitation of the acceleration rate in the previous schemes, recent studies have shown that higher acceleration rates can be achieved using compressed-sensing (CS) compared to more established techniques such as parallel imaging (13-15). In a study by Tao et al. (13), CS reconstruction was simulated with retrospectively gated 2D PC cine scans of carotid blood flow. The study by Hsiao et al. (14) assessed the accuracy of flow quantification for 4D phase contrast MRI by comparing parallel imaging and CS. Kim et al. (15) performed a combination of spatio-temporal (k-t)-based CS and parallel imaging, called k-t SPARSE-SENSE for prospectively under-sampled *in-vivo* data, and reported agreements between k-t SPARSE-SENSE and GRAPPA. While k-t approaches could surpass the acceleration achievable using acceleration in the spatial domain alone, it could also cause temporal blurring. Stadlbauer et al. (16) demonstrated that 6-fold k-t BLAST shows a reduction in peak velocity compared to rate 2 SENSE, which is caused by temporal blurring. Therefore, alternative methods are needed that can enable acceleration without temporal blurring.

In this study, we sought to develop and evaluate a new accelerated PC CMR approach in which the sparsity of the complex difference image for each individual phase is used as an additional sparsifying transform in compressed-sensing reconstruction for the quantitative evaluation of flow. Initially, the accuracy of the proposed reconstruction algorithm is evaluated by retrospectively discarding data from the fully-sampled k-space. Subsequently, accelerated data acquisition is performed in a cohort of healthy subjects to evaluate the accuracy and reproducibility of the proposed accelerated data acquisition and reconstruction.

THEORY

PC MR images are typically reconstructed using the phase difference between the two image data sets with different bipolar encoding gradients. Assuming the bipolar gradient is applied for the slice selection gradient, the complex MR signal $s_1(k_x, k_y)$ from a moving

magnetization $m_1(x,y)$ with velocity vector $v_z(x,y)$ in the z-direction for each point in the x-y plane can be expressed as:

$$s_1(k_x,k_y)=\iint_{x,y} m_1(x,y)e^{-i[2\pi(k_x x+k_y y)-\gamma M_z v_z(x,y)]}dxdy \quad [1]$$

where M_z is the first moment of the bipolar gradient and γ is the gyromagnetic ratio. For the second scan with the other bipolar gradient, we get

$$s_2(k_x,k_y)=\iint_{x,y} m_2(x,y)e^{-i[2\pi(k_x x+k_y y)+\gamma M_z v_z(x,y)]}dxdy. \quad [2]$$

The phase difference images are reconstructed using the following equation:

$$\begin{gathered} z_1=m_1e^{i\gamma M_z v_z}, z_2=m_2e^{-i\gamma M_z v_z} \\ \Delta\varphi=angle(z_1\times z_2^*)=2\gamma M_z v_z \end{gathered} \quad [3]$$

The phase difference method is commonly used to quantitatively assess the blood volume/velocity through a vessel of interest. An alternative method for processing the PC data is complex difference (CD) processing (17). In this technique, a CD image is calculated using:

$$CD=z_1-z_2=m_1e^{i\gamma M_z v_z}-m_2e^{-i\gamma M_z v_z}\approx m_1(e^{i\gamma M_z v_z}-e^{-i\gamma M_z v_z}) \quad [4]$$

where m_1 is assumed to be identical to m_2. The signal in the CD image depends on the blood flow in a voxel. For stationary voxels, the signal difference between the two acquisitions is almost zero. Therefore, the CD image contains signal only in locations where there is blood flow resulting in a very sparse image. We will utilize the sparsity of the CD image in the proposed reconstruction strategy.

Compressed Sensing for Phase Contrast MR

For PC CMR, CS reconstruction is conventionally performed simply by solving a pair of unconstrained optimization problems for each individual bipolar encoding image m_i:

$$\begin{gathered} \underset{z_1}{arg\,min}\|F_\Omega z_1-s_1\|_2+\lambda\|\Psi z_1\|_1 \\ \underset{z_2}{arg\,min}\|F_\Omega z_2-s_2\|_2+\lambda\|\Psi z_2\|_1 \end{gathered} \quad [5]$$

where F_Ω is the Fourier transform with under-sampling, Ψ is a sparsifying transform, s_i is the measurement for each of the two bipolar encodings with i = 1 or 2, z_i is the respective complex image, and λ is the weight of the sparsity terms.

In this study, we exploit an additional constraint for reconstructing phase contrast MRI in which the sparsity of the complex difference image is used in addition to the decoupled objective functions in [5]. In this case, the objective function is given by:

$$J(z_1,z_2)=\|F_\Omega z_1-s_1\|_2+\|F_\Omega z_2-s_2\|_2+\lambda\|\Psi z_1\|_1+\lambda\|\Psi z_2\|_1+\lambda_{CD}\|z_1-z_2\|_1, \quad [6]$$

where $|\boldsymbol{z}_1 - \boldsymbol{z}_2|$ is the complex difference (CD) image and λ and λ_{CD} are the regularization parameters for balancing between data fidelity and image sparsity. In our optimization procedure, we use an alternating minimization approach (24), to solve [6] as two optimization problems over each image individually at each iteration:

Initialize $z_2^0 = 0$, and $k = 0$;

While "not converged," **Do**

(step 1) Fix $\boldsymbol{z}_2 = \boldsymbol{z}_2^{\boldsymbol{k}}$ and minimize $\boldsymbol{J}(z_1, z_2^{\boldsymbol{k}})$ in terms of $\boldsymbol{z}_1$ and let $\boldsymbol{z}_1^{\boldsymbol{k}} = \boldsymbol{z}_1$.

(step 2) Fix $\boldsymbol{z}_1 = \boldsymbol{z}_1^{\boldsymbol{k}}$ and minimize $\boldsymbol{J}(z_1^{\boldsymbol{k}}, z_2)$ in terms of $\boldsymbol{z}_2$ and let $\boldsymbol{z}_1^{\boldsymbol{k}+1} = \boldsymbol{z}_2$.

(step 3) $k = k + 1$

End Do

MATERIALS AND METHODS

All images were obtained using 1.5-T Achieva magnet (Philips Healthcare, Best, The Netherlands) with a 5-channel cardiac coil. The acquired MR data were transported to a stand-alone computer and the image reconstruction was performed off-line using customized software developed in MATLAB (The MathWorks, Inc., Natick, MA, USA). All *in-vivo* studies were approved by our institutional review board, and subjects provided written consent prior to participating in the study.

This study involves two steps. Initially, we evaluated the proposed reconstruction method by quantifying flow for different acceleration rates using retrospectively under-sampled data from fully-sampled acquisitions. We also determined the optimum set of reconstruction parameters, which were used in the subsequent study step with a prospectively under-sampled image acquisition, where the accuracy of the accelerated acquisition was studied.

Image Acquisition

Phase contrast images were acquired using an axial slice of the ascending aorta at the level of the bifurcation of the pulmonary artery. For the retrospective under-sampling study, a prospectively ECG-triggered flow-encoded 2D PC cine MRI pulse gradient-echo imaging sequence was used with typical parameters of: FOV = 320×400 mm^2, resolution = 2.5×2.5 mm^2, acquisition matrix = 128 × 160, slice thickness = 8 mm, TR/TE = 4.6/2.7 ms, flip angle = 12°, temporal resolution = 28.3~39.1 ms, and VENC = 300 cm/s. The fully-sampled k-space data were acquired in 15 healthy adult subjects (5 males, range: 20-70 years). The data were retrospectively under-sampled for various acceleration rates (R = 2, 3, 4, and 5) by randomly discarding outer k-space lines while keeping the center of k-space. The size of the central k-space was set to be half of the size of the total number of k-space lines acquired at that acceleration rate. To allow a sufficient number of k-space lines around the center, we did not fix the size of the center of k-space for different acceleration rates.

Subsequently, accelerated PC CMR was acquired in 11 subjects (4 males, range: 20-45 years) with the same imaging parameters as described above. To enable accelerated data acquisition with a random under-sampling pattern, the imaging pulse sequence was modified

such that a fully-sampled central k-space (40, 26, 20, 16, and 14 k_y lines out of total 160 k_y lines for acceleration rates of 2, 3, 4, 5, and 6 respectively) was acquired, and the remaining edges of the k-space were sampled randomly until a sufficient number of lines were acquired for a given acceleration rate. A modified low-to-high profile ordering was used to minimize artifacts due to rapid gradient switching (18, 19). Each subject was imaged with acceleration rates (R) of 1 (i.e. fully-sampled) to 6. To assess the inter-scan variability, each scan was repeated twice, one after the other. In summary, each subject was imaged 12 times using 6 acceleration rates (R1 to R6) with one repeat scan for each acceleration rate.

Image reconstruction

The image reconstruction was performed according to algorithm presented in Figure 1, which illustrates how the proposed CS reconstruction procedure utilizes the sparsity of the CD image and alternating minimization. Initially, estimates of $\hat{z}_1$ and $\hat{z}_2$ are both set to all-zero images. Then, at each iteration, the algorithm keeps $\hat{z}_2$ fixed, and solves the first line of [6] for an estimate $\hat{z}_1$ by performing the data fidelity procedure and the thresholding procedure using both the first sparsity term $\|\Psi z_1\|_1$ and the additional sparsity of the CD image $|z_1 - \hat{z}_2|$. Then $\hat{z}_1$ is kept fixed, and the second line of [6] is solved for $\hat{z}_2$ using both $\|\Psi z_2\|_1$ and the sparsity of the CD image $|\hat{z}_1 - z_2|$ similarly. This is repeated until convergence, defined as when the relative change of the norm of both images becomes less than 5×10^{-4}. Total variation (TV) regularization was performed as the sparsifying transform, Ψ, since TV was shown to be a good constraint for noise removal in image restoration in (20) and has been widely used in many CS MR studies in (21,22). The reconstruction of each image is performed coil by coil using the fast alternating direction method for TVL1-L2 minimization (23). Using these two complex images, $\hat{z}_1$ and $\hat{z}_2$, we extract the flow information from the phase difference reconstruction. The reconstruction procedure described above can be considered as an alternating minimization formulation to solve the optimization problem involving the sum of the two objective functions (24).

The proposed reconstruction algorithm with CS is applied separately for all cardiac phases, which adds computational complexity to the reconstruction. The CD image in cardiac phases where there is minimal blood flow does not contain any information except velocity noise resulting from the dominant phase error, and the image also does not add any additional information to improve the reconstruction. Figure 2 shows the CD images for all 25 cardiac phases of a healthy subject. In the CD images of the first 10 phases, vessels are clearly seen for the ascending and descending aortas. Therefore, CD image are used as an additional constraint for the CS algorithm for these phases. However, CD images of the latter 15 phases do not have much information about the vessel compared to the background image. Therefore there might be a chance that the thresholding operations throw out some important signals for those phases. In these cases, it is beneficial not to use the CD images for CS reconstruction in order to improve the performance and also reduce the complexity. Therefore, the additional CD constraint was only used during the time when the aortic flow was high enough for the CD image to have substantial vessel signal. We set the cardiac phases that use a CD constraint for the reconstruction as the first 40% of the whole cardiac cycle and the values of λ and λ_{CD} were set as 10^{-4}. For the latter 60% of the cardiac cycle, we set $\lambda_{CD} = 0$ and $\lambda = 10^{-4}$ to have the regular CS algorithm as given in the equation [5].

For comparison, images were also reconstructed without the use of the CD constraint throughout the cardiac cycle, as given in equation [5].

Image and Statistical Analysis

For each reconstruction, a region of interest (ROI) was manually drawn in the ascending aorta using the corresponding magnitude images. The ROI was manually corrected through the cardiac cycle for cardiac motion. The mean velocity of blood flow in each cardiac cycle and the cardiac output were calculated for each reconstruction. Bland-Altman analysis and Pearson correlation were performed to compare the cardiac outputs reconstructed by CS reconstruction with and without using the CD image as a constraint. The cardiac output calculated by the reconstruction using the fully-sampled data was used as a reference.

RESULTS

Retrospective Under-sampling

Figure 3 shows the convergence speed of the proposed reconstruction algorithm. Sample phase contrast images from a healthy subject are shown in: (a) the magnitude image, (b) the phase difference image, (c) the complex difference image reconstructed using fully-sampled k-space data; and (d-e) the corresponding CD images for different iterations (1, 16, 256 respectively) of the proposed reconstruction algorithm applied to a retrospectively 5-fold under-sampled k-space dataset of the same subject. Aliasing artifacts and blurring are clearly visible in the CD image at the start of the algorithm seen in Figure 3 (d). However, through the iterative CS reconstruction algorithm, the vessel walls get sharper, and the CD image becomes sparser, similar to the CD image of the fully-sampled data in Figure 3 (f).

Table 1 shows the cardiac output for different under-sampling rates. There is excellent agreement between rate 1 (fully-sampled data) and rate 2 (correlation coefficient: 0.999) and between rate 1 and rate 3 (correlation coefficient: 0.999). Although the Pearson correlation coefficient decreases for higher acceleration rates, it is always above 0.97, indicating good agreement between the accelerated reconstruction and the reference. The results of the study with the retrospectively under-sampled data suggest that 5-fold accelerated PC CMR utilizing the proposed CS algorithm with the sparsity of the CD image as an additional constraint is a feasible technique for the assessment of cardiac output measured through ascending aorta.

Prospective Under-sampling

Figure 4 shows the Bland-Altman analysis of the cardiac output of the prospectively accelerated acquisitions, and Table 2 summarizes the relevant mean and standard deviations of the differences between the fully-sampled data and CS reconstruction of the accelerated scan with and without use of the CD image. Figure 4(a) shows the inter-scan reproducibility of the fully-sampled data, which shows differences between two separate scans under the same scan condition. Figure 4(b-f) shows agreement between a fully-sampled acquisition and the accelerated acquisitions for rates 2-6. The figure also compares two different CS algorithms, one which utilizes CD sparsity and another one that does not. Black squares and black solid lines indicate that the variation of the difference between a fully-sampled scan

and an accelerated scan reconstructed with the proposed algorithm is in the range of that of the scan-rescan of the fully-sampled data up to acceleration rate 4. The variation is also in the acceptable range with rate 5. However, there is a larger variation (by 98% compared to the reproducibility of the fully-sampled data) in the flow measurement for rate 6 as seen in Table 2. Furthermore, larger standard deviations are observed in the difference between the fully-sampled scan and accelerated scan reconstructed without the CD constraint, especially for high acceleration rates (12% and 19% increase for rates 4 and 5 respectively compared to the reconstruction with the CD constraint) as depicted in Table 2. We note that these differences are more positively biased for the case of the CS without the CD constraint, which would lead to greater underestimation of the velocity of the blood.

Figure 5 depicts the inter-scan reproducibility of the CS reconstruction with the CD constraint. Figure 5(a) shows the inter-scan reproducibility of the fully-sampled data, and Figure 5(b-f) shows those of the accelerated acquisitions for rates 2 to 6, respectively. Up to acceleration rate 5, the ranges of the standard deviations are not bigger than that of the reference in Figure 5(a). The standard deviation of Figure 5(f) is comparatively higher than Figure 5(a).

DISCUSSION

We introduced a novel CS reconstruction algorithm for accelerated phase contrast CMR. The sparsity of the CD image was included as an additional constraint for the minimization problem in this approach. No systematic variation was observed for the cardiac output measurements between the fully-sampled reference data and those reconstructed with the proposed reconstruction algorithm up to acceleration rate 5.

In previous studies on the utility of CS in accelerated PC MR, underestimation of the velocities of voxels of interest was noted as an issue (14, 15). Underestimation can be seen as the bias of the Bland-Altman analysis comparing fully-sampled PC acquisition and reconstructions of the accelerated PC acquisitions. We also showed that the CS reconstruction which uses total variation of the image without CD sparsity suffered from the underestimation of the cardiac output as seen by the positive bias of the difference. However, by utilizing the CD image and an additional sparsifying constraint, the bias of the difference of the cardiac output was significantly reduced for acceleration rates of up to 5.

One of the major issues for CS is the loss of spatial resolution or blurring of the reconstructed image. Over the past years, there have been various improved reconstructions that address this issue for high-resolution cardiac MRI (19,25,26). However, for PC imaging, the issue of blurring has less impact on quantification of the flow. First, the spatial resolution is much lower than needed for the assessment of coronary lesions or scar. Second, during the analysis, we intentionally avoid pixels in the vessel wall to reduce the partial volume errors. Third, quantification of flow is usually performed over the entire cardiac cycle using average blood flow velocity. The maximum achievable acceleration rate will also depend on the imaging spatial resolution as well as vessel diameter, therefore the maximum achievable acceleration rate for each imaging application might be different from the ones reported in our study. Further studies in larger cohorts and in patients with valvular

disease should be performed to further validate the impact of CS in acceleration of PC CMR.

The per-iteration computational cost of the proposed algorithm is four FFTs (including two inverse FFTs) and four thresholding operations, all applied to images of the size of the 2D phase image. The reconstruction time is dependent on the actual number of cardiac phases and the required number of iterations but it is approximately less than 20 minutes using MATLAB on a 64-bit windows PC with dual core CPU and 8GB of RAM. The reconstruction time may be further reduced to a clinically acceptable range through the use of parallel programming and a graphics processing unit (27).

In our study, we have chosen to use the additional sparsity of the CD image in the first 40% of the cardiac cycle. The CD images show very little flow-related information at later cardiac phases due to the lack of large flow during these cardiac cycles. For assessment of flow in other vasculature, CD sparsity may be used throughout the entire cardiac cycle.

In our study, different image reconstruction techniques are compared based on cardiac output measurements. Although cardiac output is a valuable quantitative metric for PC CMR, it is not necessarily sensitive to subtle changes and artifacts in the flow pattern. Therefore, further evaluation in other PC CMR applications should be performed using clinically relevant metrics for each specific application.

In our study, the maximum acceleration rate was limited to 5 and the proposed scheme was not feasible with a rate of 6 or higher. Higher acceleration rates may be possible with a larger number of coil elements, since images will be better localized in different coils, although this was not studied. The optimal combination of our technique with parallel imaging was also not studied. We have used an arbitrary size of the center of k-space to be fully sampled. The optimal size for the fully-centered k-space was not systematically studied and may be different from the one we chose in this study. We also note there was a previous study on CS for PC utilizing the CD image (28) for MR angiography with maximum intensity projection images in the brain, but not for flow assessment.

Our study has some limitations. Only subjects with no prior history of cardiovascular disease were recruited. Further validations in patients with cardiac disease are needed to evaluate the accuracy of the accelerated flow measurements with complex difference sparsity. We have only used total variation in the reconstruction and did not study other sparsyfing transform such as wavelet in the reconstruction. We also used a uniform random undersampling instead of weighted sampling in our data acquisition to reduce computational time of calculating the undersampling pattern in real-time for implementation of the prospective under-sampling acqusition. The impact of different reconstruction on resolution loss of the magnitude images were not studied.

CONCLUSION

Complex difference images, calculated from two bipolar encoding acquisitions of phase contrast cine, can be used as additional sparsifying constraints in compressed sensing

reconstructions allowing higher acceleration rates with lower variations in flow measurements.

Acknowledgments

The authors would like to thank Jaime L. Shaw for proof-reading the manuscript.

The project described was supported by NIH R01EB008743-01A2, Samsung Electronics and NIH UL1 RR025758-01, Harvard Clinical and Translational Science Center, from the National Center for Research Resources.

References

1. Nayler GL, Firmin DN, Longmore DB. Blood flow imaging by cine magnetic resonance. J Comput Assist Tomogr. 1986; 10(5):715–722. [PubMed: 3528245]
2. Pelc NJ, Herfkens RJ, Shimakawa A, Enzmann DR. Phase contrast cine magnetic resonance imaging. Magn Reson Q. 1991; 7(4):229–254. [PubMed: 1790111]
3. Rebergen SA, van der Wall EE, Doornbos J, de Roos A. Magnetic resonance measurement of velocity and flow: technique, validation, and cardiovascular applications. Am Heart J. 1993; 126(6): 1439–1456. [PubMed: 8249802]
4. Markl M, Chan FP, Alley MT, Wedding KL, Draney MT, Elkins CJ, Parker DW, Wicker R, Taylor CA, Herfkens RJ, Pelc NJ. Time-resolved three-dimensional phase-contrast MRI. J Magn Reson Imaging. 2003; 17(4):499–506. [PubMed: 12655592]
5. Ordidge RJ, Mansfield P, Doyle M. Real time movie images by NMR. British Journal of Radiology. 1982; 55(658):729–733. [PubMed: 7127023]
6. Nayak KS, Pauly JM, Kerr AB, Hu BS, Nishimura DG. Real-time color flow MRI. Magn Reson Med. 2000; 43(2):251–258. [PubMed: 10680689]
7. Park JB, Olcott EW, Nishimura DG. Rapid measurement of time-averaged blood flow using ungated spiral phase-contrast. Magn Reson Med. 2003; 49(2):322–328. [PubMed: 12541253]
8. Barger AV, Peters DC, Block WF, Vigen KK, Korosec FR, Grist TM, Mistretta CA. Phase-contrast with interleaved undersampled projections. Magn Reson Med. 2000; 43(4):503–509. [PubMed: 10748424]
9. Pruessmann KP, Weiger M, Scheidegger MB, Boesiger P. SENSE: sensitivity encoding for fast MRI. Magn Reson Med. 1999; 42(5):952–962. [PubMed: 10542355]
10. Griswold MA, Jakob PM, Heidemann RM, Nittka M, Jellus V, Wang J, Kiefer B, Haase A. Generalized autocalibrating partially parallel acquisitions (GRAPPA). Magn Reson Med. 2002; 47(6):1202–1210. [PubMed: 12111967]
11. Thunberg P, Karlsson M, Wigstrom L. Accuracy and reproducibility in phase contrast imaging using SENSE. Magn Reson Med. 2003; 50(5):1061–1068. [PubMed: 14587017]
12. Baltes C, Kozerke S, Hansen MS, Pruessmann KP, Tsao J, Boesiger P. Accelerating cine phase-contrast flow measurements using k-t BLAST and k-t SENSE. Magn Reson Med. 2005; 54(6): 1430–1438. [PubMed: 16276492]
13. Tao, Y.; Rilling, G.; Davies, M.; Marshall, I. Compressed sensing reconstruction with retrospectively gated sampling patterns for velocity measurement of carotid blood flow. Proceedings of the 18th Annual Meeting of ISMRM; Stockholm, Sweden. 2010. p. 4866
14. Hsiao, A.; Lustig, M.; Alley, MT.; Murphy, M.; Vasanawala, SS. Quantitative assessment of blood flow with 4D phase-contrast MRI and autocalibrating parallel imaging compressed sensing. Proceedings of the 19th Annual Meeting of ISMRM; Montreal, Canada. 2011. p. 1190
15. Kim D, Dyvorne HA, Otazo R, Feng L, Sodickson DK, Lee VS. Accelerated phase-contrast cine MRI using k-t SPARSE-SENSE. Magn Reson Med. 2012; 67(4):1054–1064. [PubMed: 22083998]
16. Stadlbauer A, van der Riet W, Crelier G, Salomonowitz E. Accelerated time-resolved three-dimensional MR velocity mapping of blood flow patterns in the aorta using SENSE and k-t BLAST. Eur J Radiol. 2010; 75(1):e15–21. [PubMed: 19581063]

17. Dumoulin CL, Souza SP, Walker MF, Wagle W. Three-dimensional phase contrast angiography. Magn Reson Med. 1989; 9(1):139–149. [PubMed: 2709992]

18. Basha, TA.; Akçakaya, M.; Moghari, MH.; Kissinger, KV.; Goddu, B.; Goephert, L.; Manning, WJ.; Nezafat, R. Minimization of Imaging Artifacts from Profile Ordering of Randomly Selected ky-kz Lines for Prospective Compressed-Sensing Acqusition in 3D Segmented SSFP and GRE Imaging. Proceedings of the 19th Annual Meeting of ISMRM; Montreal, Canada. 2011. p. 1264

19. Akcakaya M, Basha TA, Chan RH, Rayatzadeh H, Kissinger KV, Goddu B, Goepfert LA, Manning WJ, Nezafat R. Accelerated contrast-enhanced whole-heart coronary MRI using low-dimensional-structure self-learning and thresholding. Magn Reson Med. 2012; 67(5):1434–1443. [PubMed: 22392654]

20. Rudin LI, Osher S, Fatemi E. Nonlinear total variation based noise removal algorithms. Physica D: Nonlinear Phenomena. 1992; 60(1–4):259–268.

21. Lustig M, Donoho D, Pauly JM. Sparse MRI: The application of compressed sensing for rapid MR imaging. Magn Reson Med. 2007; 58(6):1182–1195. [PubMed: 17969013]

22. Block KT, Uecker M, Frahm J. Undersampled radial MRI with multiple coils. Iterative image reconstruction using a total variation constraint. Magn Reson Med. 2007; 57(6):1086–1098. [PubMed: 17534903]

23. Junfeng Y, Yin Z, Wotao Y. A fast alternating direction method for TVL1-L2 signal reconstruction from partial fourier data. Selected Topics in Signal Processing, IEEE Journal of. 2010; 4(2):288–297.

24. Wang Y, Yang J, Yin W, Zhang Y. A New Alternating Minimization Algorithm for Total Variation Image Reconstruction. SIAM Journal on Imaging Sciences. 2008; 1(3):248–272.

25. Akcakaya M, Basha TA, Goddu B, Goepfert LA, Kissinger KV, Tarokh V, Manning WJ, Nezafat R. Low-dimensional-structure self-learning and thresholding: regularization beyond compressed sensing for MRI reconstruction. Magn Reson Med. 2011; 66(3):756–767. [PubMed: 21465542]

26. Akcakaya M, Rayatzadeh H, Basha TA, Hong SN, Chan RH, Kissinger KV, Hauser M, Josephson E, Manning WJ, Nezafat R. Accelerated Late Gadolinium Enhancement Cardiac MRI with Isotropic Spatial Resolution Using Compressed Sensing: Initial Experience. Radiology. 2012 Epub ahead of print.

27. Nam S, Akcakaya M, Basha T, Stehning C, Manning WJ, Tarokh V, Nezafat R. Compressed sensing reconstruction for whole-heart imaging with 3D radial trajectories: A graphics processing unit implementation. Magn Reson Med. 2012 Epub ahead of print. 10.1002/mrm.24234

28. King, KF.; Sun, W. Compressed sensing with vascular phase contrast acquisition. Proceedings of the 17th Annual Meeting of ISMRM; Honolulu, USA. 2009. p. 2817

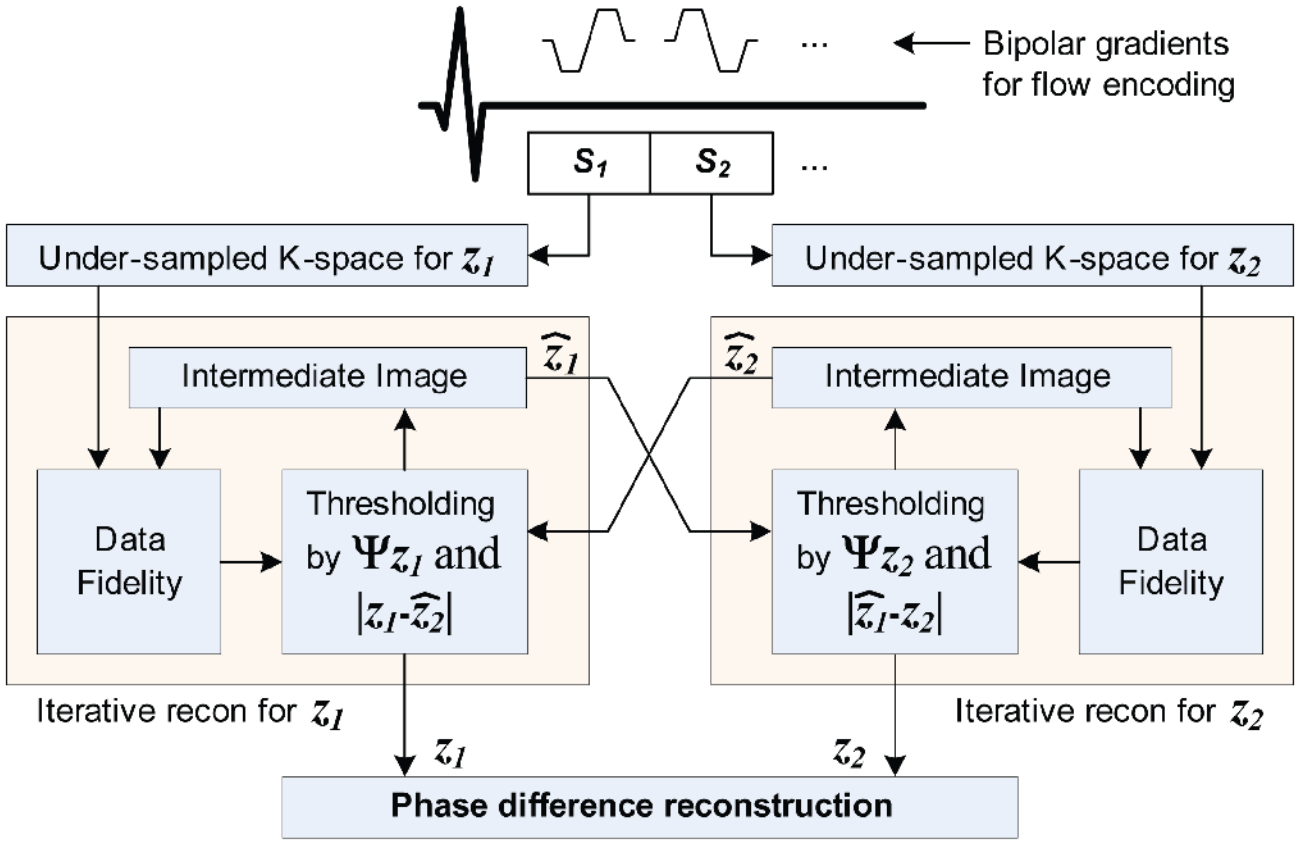

Figure 1.

Iterative compressed sensing (CS) reconstruction of the phase contrast MR using the sparsity of the complex difference image. The reconstruction consists of two separate iterative processes, each with two steps of data fidelity and thresholding. The thresholding step utilizes both the sparsifying transform of the image (Ψz_i) and the intermediate image of the other process for calculating the complex difference image. The unaliased phase difference image is then obtained using final estimation of $\boldsymbol{z_1}$ and $\boldsymbol{z_2}$.

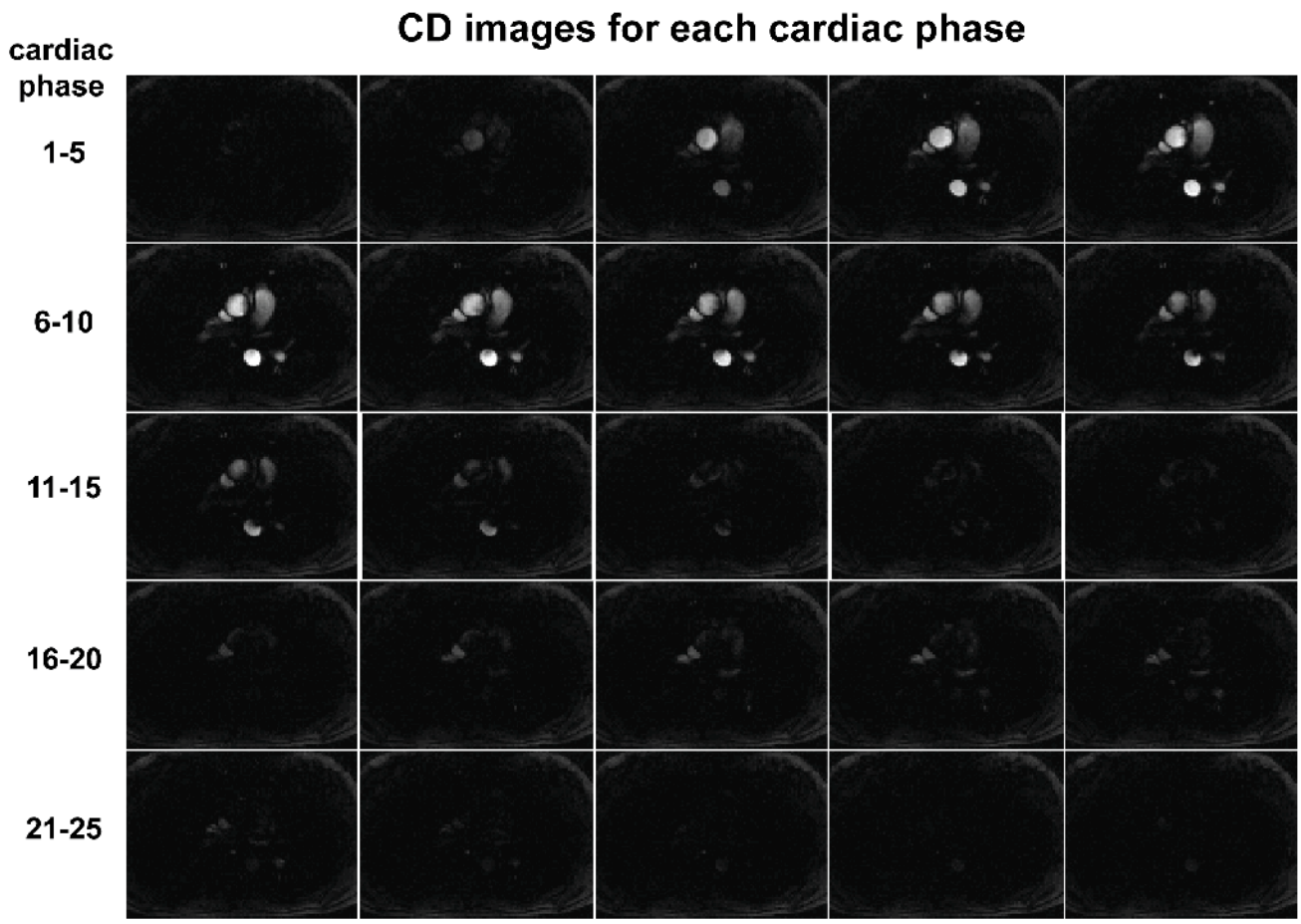

Figure 2.

Magnitude images of the complex difference (CD image) for 25 cardiac phases. CD images of the early 10 phases show clear vessels for ascending and descending aorta, and the sparsity of the CD image can be used as an additional constraint for the CS algorithm. CD images of the latter 15 phases do not contain vessel signal above the noise level, hence there is no benefit in using CD images for the CS reconstruction for these phases.

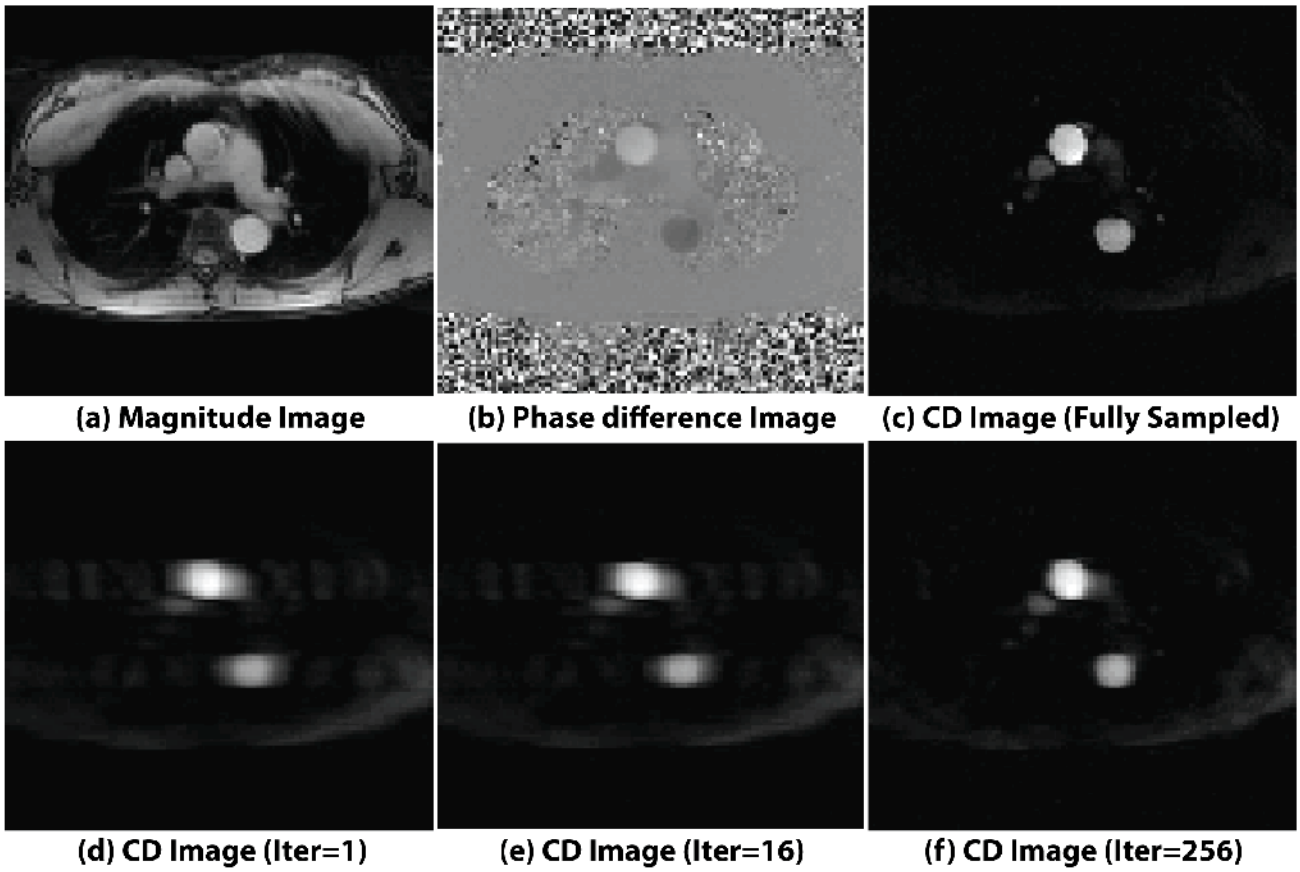

Figure 3.

The first row shows fully-sampled images of an axial slice of the ascending aorta at the level of the bifurcation of the pulmonary artery: (a) magnitude image, (b) phase difference image, and (c) CD image. The images in the second row (d-f) are the corresponding CD images from different iterations of the CS algorithm (1, 16 and 256) for a retrospectively under-sampled acquisition of acceleration rate 5. Improved depiction of vessel boundaries can be seen in later iterations.

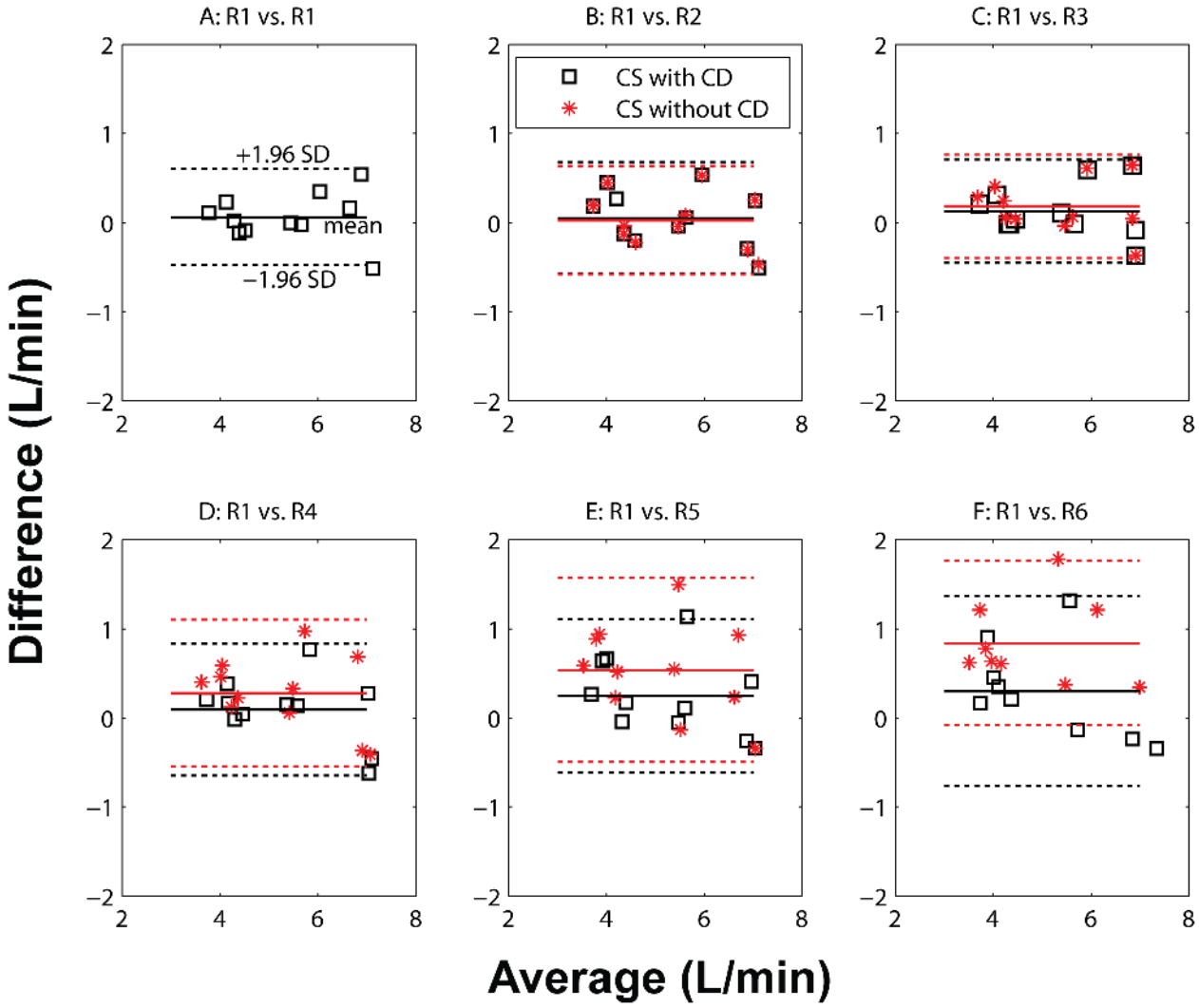

Figure 4.

Bland-Altman analysis of the blood volume through the ascending aorta for scan/rescan variability of (a) the fully-sampled acquisitions (R1 vs. R1), and (b-f) the comparison between the fully-sampled data and reconstructions of prospectively accelerated scan with rates (R) of 2 to 6 using: 1) CS with CD sparsity (black square) and 2) CS without CD sparsity (red star) for a. At lower rates (R≤3), both reconstruction techniques yield clinically equivalent results. However, at higher acceleration rates, CS reconstruction with CD sparsity results in superior flow measurements and smaller differences than the CS reconstruction without CD sparsity, when compared to the fully-sampled acquisition.

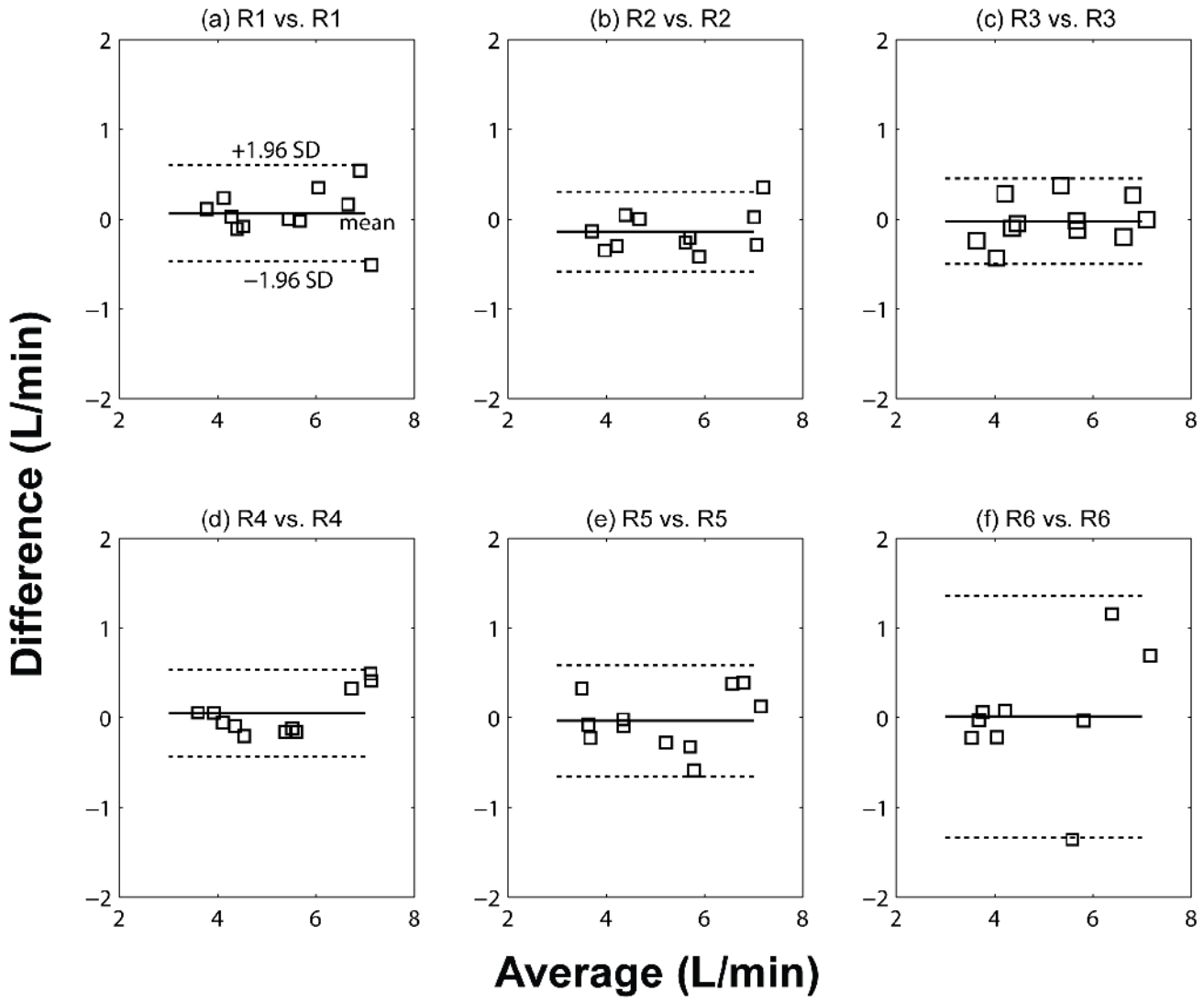

Figure 5.

Bland-Altman analysis of the blood volume through the ascending aorta for scan/rescan variability of (a) fully-sampled acquisitions (R1 vs. R1), and (b-f) prospectively accelerated scans with rates (R) of 2 to 6 using CS reconstructions with CD sparsity. At acceleration rates ≤5, the proposed reconstruction technique yields clinically equivalent results with the fully-sampled acquisitions.

Table 1

Bland-Altman analysis of the cardiac output between the fully-sampled data and CS reconstruction of the retrospectively under-sampled data and relevant Pearson coefficients, R.

Acceleration Rate (R)	Mean of difference (L/min)	Upper 95% (L/min)	Lower 95% (L/min)	Pearson Coefficients R
2	-0.004	0.120	-0.129	0.999
3	0.018	0.152	-0.117	0.999
4	0.052	0.429	-0.326	0.991
5	0.153	0.867	-0.562	0.970

Table 2

Bland-Altman analysis of the cardiac output between the fully-sampled data and two difference CS reconstructions with and without use of CD constraint for the prospectively under-sampled data.

Acceleration Rate (R)	Use of CD constraint	Mean of difference (L/min)	SD of difference (L/min)	Upper 95% (L/min)	Lower 95% (L/min)
R1 vs. R1	N/A	0.0623	0.273	0.598	-0.474
R1 vs. R2	with CD	0.0530	0.319	0.678	-0.572
	without CD	0.0286	0.309	0.633	-0.576
R1 vs. R3	with CD	0.128	0.295	0.706	-0.449
	without CD	0.182	0.295	0.761	-0.396
R1 vs. R4	with CD	0.0930	0.378	0.833	-0.647
	without CD	0.280	0.421	1.11	-0.545
R1 vs. R5	with CD	0.246	0.441	1.11	-0.618
	without CD	0.536	0.526	1.57	-0.496
R1 vs. R6	with CD	0.299	0.542	1.36	-0.763
	without CD	0.841	0.470	1.76	-0.0790